Majorana bound states in a disordered quantum dot-superconductor chain

P. Zhang[1] and Franco Nori[1,2]

[1]*CEMS, RIKEN, Saitama 351-0198, Japan*

[2]*Department of Physics, The University of Michigan, Ann Arbor, Michigan 48109-1040, USA*

(Dated: January 8, 2016)

We study Majorana bound states in a disordered chain of semiconductor quantum dots connected to each other by s-wave superconductors. By calculating its topological quantum number, based on the scattering matrix method in the framework of a tight-binding model, we can identify the topological property of such an inhomogeneous one dimensional system. We study the robustness of Majorana bound states against disorder in both the spin-independent terms (including the chemical potential and the regular spin-conserving hopping) and the spin-dependent term, i.e., the spin-flip hopping due to the Rashba spin-orbit coupling. We find that the Majorana bound states are *not* completely immune to the spin-independent disorder, especially when the latter is strong. Meanwhile, the Majorana bound states are relatively robust against the spin-dependent disorder, as long as the spin-flip hopping is sign-ordered. Nevertheless, when the disorder induces sign-flip in spin-flip hopping, the topological-nontopological phase transition tends to take place in the low chemical potential region.

PACS numbers: 71.10.Pm, 74.78.Na

I. INTRODUCTION

Majorana bound states (MBS)[1,2] in solid-state systems are recently attracting increasing interest, both theoretically and experimentally. Being first proposed by Kitaev more than 10 years ago in a spinless toy model,[1] these zero-energy bound states are expected to exist in several structures with spin, including nanowires with spin-orbit coupling (SOC) in proximity to a superconductor (SC),[3,4] ferromagnetic atom chains on top of a SC,[5] topological insulator/SC hybrid structures,[6–11] quantum dot (QD)-SC chains,[12–14] as well as cold-atom systems.[15] Experimentally, possible signatures of MBS have been reported in nanowires,[16–18] atom chains,[19] and topological insulator/SC structures.[20]

Majorana bound states attract considerable attention partly due to their future potential applications in quantum information.[2,21–23] One attractive possibility would be to construct Majorana qubits based on MBS.[21] Majorana qubits, among various qubit candidates,[24–30] are suggested to be robust against local perturbations and hence promising to store quantum information.[12,21,31] Moreover, arbitrary qubit rotations are expected to be implemented, by means of topologically-protected braiding operations[22,32] in combination with other nontopological operations assisted by, e.g., nanomechanical resonators.[33,34] However, recent studies reveal that the MBS are not completely robust against disorder in both the Kitaev's spinless model and the systems with spin,[35–40] and the Majorana qubit is also not totally protected from decoherence.[41–44] Note that the studies investigating so far the effect of disorder on MBS focus solely on the spin-independent disorder, without considering the spin-depenent one. In fact, the spin-dependent disorder, e.g., the fluctuation in SOC, can be present inevitably in many solid-state systems and play an important role in the spin-related dynamics.[45,46] Therefore, the effect of spin-dependent disorder on the existence of MBS deserves to be investigated.

In this work, we systematically study the robustness of MBS against disorder, based on a concrete structure, i.e., a QD-SC chain.[12–14] Experimentally, such a QD-SC chain system might have the advantage to be adaptively tuned, as suggested in Refs. 12 and 13. However, in the absence of precise control, this system is also very likely to be disordered due to, e.g., the inhomogeneity in QD/SC sizes or QD confining potentials. Therefore, we take a QD-SC chain as an ideal platform to look into the influence of disorder. Concretely, we calculate the topological quantum number by means of the scattering matrix method based on a tight-binding model, to identify the topological property of a disordered chain in a relatively large parameter region. Apart from the disorder in the spin-independent terms (including the chemical potential and the regular spin-conserving hopping), we also consider the disorder in the spin-dependent term, i.e., the spin-flip hopping due to the Rashba SOC. We find that the MBS are *not* completely immune to the disorder in spin-independent terms, especially when the disorder is strong. Meanwhile, the MBS are relatively robust against the disorder in spin-flip hopping, as long as the spin-flip hopping is sign-ordered. Nevertheless, when the disorder induces sign-flip in spin-flip hopping, a topological-nontopological phase transition in the QD-SC chain tends to take place in the low chemical potential region.

This paper is organized as follows. First, we describe the inhomogeneous QD-SC chain in a tight-binding model. Then we present the scattering matrix method utilized to calculate the topological quantum number. Afterwards, we numerically study the robustness of the MBS against disorder in the QD-SC chain. Finally, we summarize our results.

II. MODEL AND HAMILTONIAN

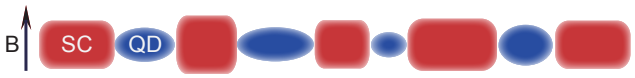

FIG. 1: (Color online) Schematic diagram of a disordered chain of semiconductor quantum dots (shown in blue) coupled by s-wave superconductors (in red), under a transverse magnetic field B. The on-site chemical potentials, spin-independent hopping terms, as well as the spin-flip hopping terms due to the Rashba SOC, can be disordered.

A QD-SC chain, as studied in, e.g., Refs. 12–14, is schematically shown here in Fig. 1. We assume that the QDs can be approximately treated as one dimensional along the chain-direction due to the strong transverse confinement. By further assuming that the orbital level splitting in the QDs is much larger than both the Zeeman splitting and Rashba SOC, we consider only the Kramers doublet closest to the chemical potential energy in each QD. The general form of the tight-binding Hamiltonian describing such a chain of single-level QDs is written as[13]

$$H = \frac{1}{2}\sum_{n\alpha\beta}[\mu_n\delta_{\alpha\beta} + B(\sigma_z)_{\alpha\beta}]f^\dagger_{n\alpha}f_{n\beta} + \Delta\sum_n f^\dagger_{n\uparrow}f^\dagger_{n\downarrow} + \sum_{n\alpha\beta}[t_n\delta_{\alpha\beta} + it^{\rm so}_n(\sigma_y)_{\alpha\beta}]f^\dagger_{n\alpha}f_{n+1\beta} + \text{H.c.}. \quad (1)$$

In the Bogoliubov-de Gennes basis $\Psi_n = (f_{n\uparrow}, f_{n\downarrow}, f^\dagger_{n\downarrow}, -f^\dagger_{n\uparrow})$, this Hamiltonian can be rewritten as[5]

$$H = \frac{1}{2}\sum_n[\Psi^\dagger_n\hat{h}_n\Psi_n + (\Psi^\dagger_n\hat{t}_n\Psi_{n+1} + \text{H.c.})], \quad (2)$$

where

$$\hat{h}_n = \mu_n\sigma_0\tau_z + B\sigma_z\tau_0 + \Delta\sigma_0\tau_x, \quad (3)$$

$$\hat{t}_n = t_n\sigma_0\tau_z + it^{\rm so}_n\sigma_y\tau_z. \quad (4)$$

In the above equations, $f^\dagger_{n\alpha}$ is the creation operator for a spin-α electron in the nth QD. The Pauli matrices $\sigma_{x,y,z}$ and $\tau_{x,y,z}$ act on the spin and particle-hole spaces, respectively. The chemical potential is labeled as μ_n. The term proportional to B is the Zeeman splitting while Δ stands for the superconducting pairing due to the proximity effect. The nearest-neighbour hopping term has two parts, i.e., the spin-conserving (t_n) and spin-flip ($t^{\rm so}_n$) ones. The spin-flip hopping can be caused by the SOC which supplies an effective magnetic field during hopping. Here we only consider the Rashba type SOC, with its effective magnetic field along the y-axis. Due to the inhomogeneity in the QD confining potentials and/or QD/SC sizes, as well as other disorder sources such as the charged impurities, both the spin-conserving terms, μ_n and t_n, and the spin-flip term, $t^{\rm so}_n$, can be QD-site dependent.

III. SCATTERING MATRIX METHOD

To identify the topological property of the QD-SC chain, we study the scattering matrix S relating the incoming and outgoing wave amplitudes at the Fermi level,[47]

$$S = \begin{pmatrix} R & T' \\ T & R' \end{pmatrix}. \quad (5)$$

In the above the 4×4 subblocks $\{R, R'\}$ and $\{T, T'\}$ are the reflection and transmission matrices at the two ends of the QD-SC chain, respectively. The Z_2 topological quantum number Q is given by[47]

$$Q = \text{sgn Det}(R) = \text{sgn Det}(R'). \quad (6)$$

Here, sgn denotes the sign of the determinant Det. The MBS arise at the ends of the QD-SC chain only when $Q = -1$.[47]

The scattering matrix can be obtained by the transfer matrix scheme. Based on Hamiltonian (2), the zero-energy Schrödinger equation gives[5]

$$\begin{pmatrix} \hat{t}^\dagger_n\Phi_n \\ \Phi_{n+1} \end{pmatrix} = \tilde{M}_n \begin{pmatrix} \hat{t}^\dagger_{n-1}\Phi_{n-1} \\ \Phi_n \end{pmatrix}, \quad (7)$$

where

$$\tilde{M}_n = \begin{pmatrix} 0 & \hat{t}^\dagger_n \\ -\hat{t}^{-1}_n & -\hat{t}^{-1}_n\hat{h}_n \end{pmatrix}. \quad (8)$$

Here Φ_n is a four-component vector of wave amplitudes on the nth site. The above recursive relation indicates that waves at the two ends ($n = 1$ and N) of the nanowire are related by the transfer matrix

$$\tilde{M} = \tilde{M}_N\tilde{M}_{N-1}...\tilde{M}_2\tilde{M}_1. \quad (9)$$

In the basis with right-moving and left-moving waves separated in the upper and lower four components, the transfer matrix transforms as

$$M_n = U^\dagger\tilde{M}_nU, \quad (10)$$

where

$$U = \frac{1}{\sqrt{2}}\begin{pmatrix} I & I \\ iI & -iI \end{pmatrix}. \quad (11)$$

In this basis, the reflection matrices R (R') and transmission matrices $T(T')$ in the scattering matrix S [refer to Eq. (5)] can be obtained via the relations

$$\begin{pmatrix} T \\ 0 \end{pmatrix} = M\begin{pmatrix} I \\ R \end{pmatrix}, \begin{pmatrix} R' \\ I \end{pmatrix} = M\begin{pmatrix} 0 \\ T' \end{pmatrix}, \quad (12)$$

where

$$M = M_NM_{N-1}...M_2M_1. \quad (13)$$

Finally, the calculation of the topological quantum number Q is reduced to that of the transfer matrix M. In Appendix A, we present the numerical scheme for calculating M.

IV. RESULTS

We now numerically study the topological property of the QD-SC chain. For comparison, we first look into an ideal homogeneous QD-SC chain and reproduce the topological phase reported in the literature, and then take into account disorder to investigate the robustness of the MBS.

A. Homogeneous QD-SC chain

For a homogeneous QD-SC chain, we label $\mu_n = \mu$, $t_n = t$ and $t_n^{\rm so} = t_{\rm so}$. In Fig. 2(a) we plot the phase diagram, Det(R) [refer to Eqs. (5) and (6)] versus μ and B, of a homogeneous QD-SC chain typically with $t = \Delta$ and $t_{\rm so} = 0.5\Delta$. The blue region in this figure, with Det(R) $= -1$, stands for the topological phase supporting MBS. It is found that this region is nicely enclosed by the white curve plotted in the figure, which defines the topological region of a single-band homogeneous superconducting nanowire as[48,49]

$$\sqrt{(2t-|\mu|)^2+\Delta^2} < |B| < \sqrt{(2t+|\mu|)^2+\Delta^2}. \quad (14)$$

In Fig. 2(b), we further show the energy spectrum (for clarity, we present only the lowest four states close to the zero energy) of this QD-SC chain versus μ when B is fixed. It is clearly indicated that when the QD-SC chain enters the topological region, the zero-energy states (localized at the two ends of the QD-SC chain) separated from the higher-energy bulk states arise. Note that when varying the spin-flip hopping $t_{\rm so}$, the topological phase space in Fig. 2(a) remains invariant, consistent with the feature that $t_{\rm so}$ is absent from Eq. (14).

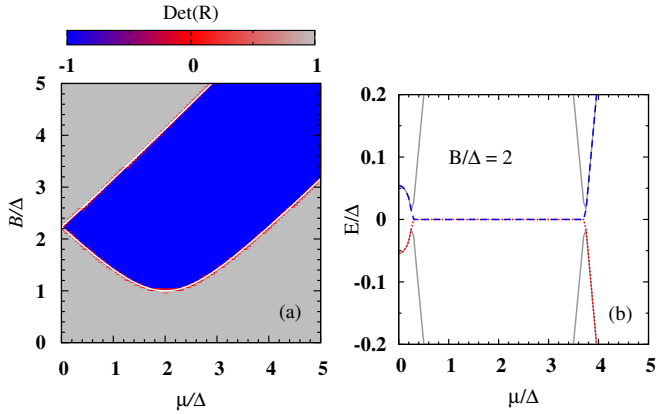

FIG. 2: (Color online) (a) The determinant Det(R) of the reflection matrix R as a function of the chemical potential μ and the Zeeman splitting B, in a homogeneous QD-SC chain with $t = \Delta$ and $t_{\rm so} = 0.5\Delta$. The blue region with Det(R) $= -1$ stands for the topological phase supporting MBS. (b) The energy spectrum (with only the lowest four eigenstates close to zero energy plotted) versus the chemical potential μ, when the Zeeman splitting B is fixed as 2Δ.

B. Inhomogeneous QD-SC chain with disordered chemical potential and spin-conserving hopping

From Eq. (14), one may infer that when the disorder is induced into the chemical potential μ or the spin-conserving hopping t_n, the topological phase space might change in the parameter space. Now we take into account such disorder to investigate the robustness of MBS in the QD-SC chain. We first consider disorder in the chemical potential, which is modeled to perturb the μ_n's independently within a uniform distribution in the interval $(\mu - \delta_\mu, \mu + \delta_\mu)$, where μ is now the mean value of the chemical potential and δ_μ stands for the fluctuation magnitude. Our calculations indicate that the topological phase is not completely immune to disorder. In Figs. 3(a) and (b), we present the phase diagrams of the inhomogeneous QD-SC chain calculated with $\delta_\mu/\Delta = 0.5$ and $\delta_\mu/\Delta = 1.5$, respectively. The comparison between these two figures indicates the effect of stronger disorder on the formation of the topological phase. To qualitatively present the effect of increasing disorder, we further study the ratio of the area of the topological region with disorder [such as the blue regions in Figs. 3(a) and (b)] to that without disorder [the region defined by Eq. (14)], labeled as λ, versus the fluctuation magnitude δ_μ. This is a qualitative study because it is performed in a finite parameter region, e.g., $0 \le \mu \le 5\Delta$ and $0 \le B \le 5\Delta$ here. The result is plotted by the solid curve with squares in Fig. 3(e). This curve shows that when the fluctuation magnitude of the chemical potential δ_μ is larger than the superconducting gap Δ, the topological phase can be effectively destroyed.

We then consider disorder in the spin-conserving hopping, with the other terms treated as uniform. We assume that the disorder causes the spin-conserving hopping to fluctuate in an interval $(t - \delta_t, t + \delta_t)$ with a uniform distribution ($\delta_t < t$). Our calculations indicate that disorder in the spin-conserving hopping can also be detrimental to the topological phase (especially when the disorder is strong), as shown by the phase diagrams in Figs. 3(c) and (d). In Fig. 3(e), by the blue curve with circles, we also plot the ratio λ of the area of the topological region for a disordered system to the one for a clean system, versus the fluctuation magnitude δ_t. Also, the stronger the disorder is, the smaller the topological phase area becomes.

C. Inhomogeneous QD-SC chain with disordered spin-flip hopping

We now focus on the robustness of the topological phase against disorder in the spin-flip hopping. Again, for simplicity, we assume that due to disorder, the spin-flip hopping fluctuates in an interval $(t_{\rm so} - \delta_{t_{\rm so}}, t_{\rm so} + \delta_{t_{\rm so}})$

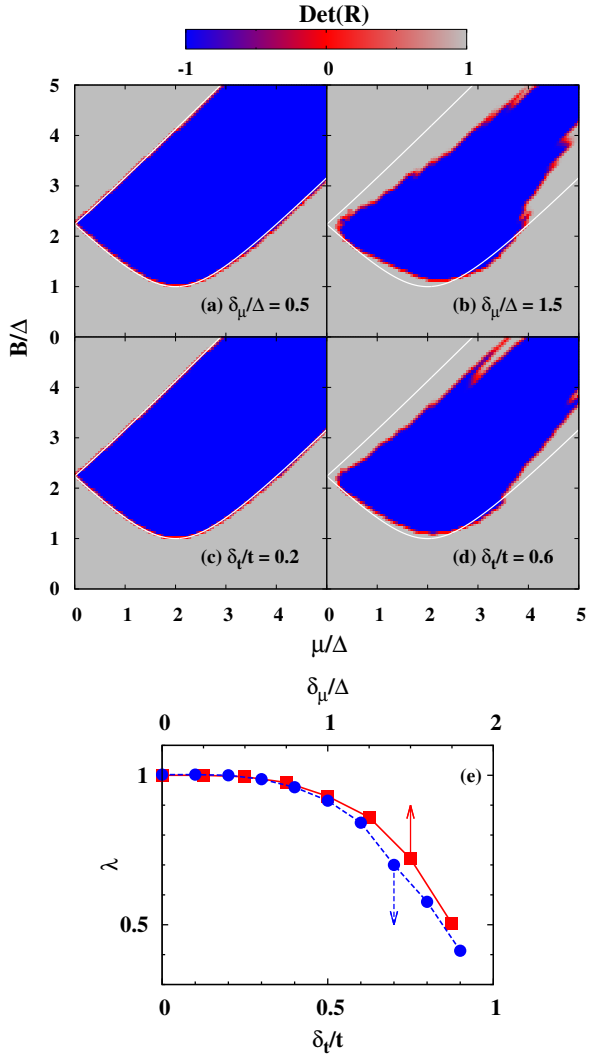

FIG. 3: (Color online) (a) and (b) [(c) and (d)] Phase diagrams of disordered QD-SC chains, where the chemical potentials μ_n (spin-conserving hoppings t_n) fluctuate in an interval $(\mu-\delta_\mu, \mu+\delta_\mu)$ $[(t-\delta_t, t+\delta_t)]$ with a uniform distribution. Note that δ_μ/Δ is set as 0.5 and 1.5, respectively, in (a) and (b), and δ_t/t is set as 0.2 and 0.6, respectively, in (c) and (d). (e) The ratio of the area of the topological region for a disordered system [such as the blue regions in (a)-(d)] to the one for a clean system [the region defined by Eq. (14), or, enclosed by the white curves in (a)-(d)], labeled as λ, versus the fluctuation magnitude δ_μ of the chemical potential μ (red curve with squares), and the fluctuation magnitude δ_t of spin-conserving hopping t (blue curve with circles). The calculations for each curve in (e) are carried out by averaging over ten disordered samples.

with a uniform distribution. We find that the topological phase is relatively robust against disorder in the spin-flip hopping, as long as the spin-flip hopping is sign-ordered (i.e., $\delta_{t_{\rm so}} < t_{\rm so}$). Nevertheless, when the disorder induces sign-flip in spin-flip hopping ($\delta_{t_{\rm so}} > t_{\rm so}$), a topological-nontopological phase transition in the QD-SC chain tends

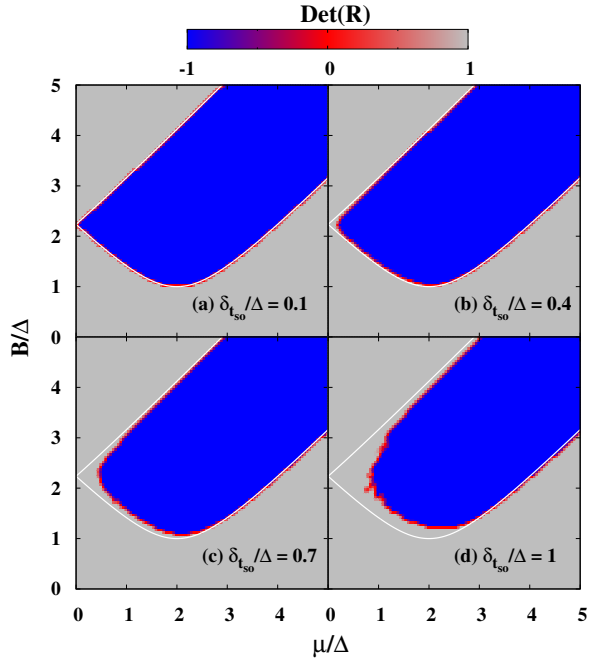

FIG. 4: (Color online) The phase diagrams of disordered QD-SC chains where the spin-flip hoppings $t_n^{\rm so}$ fluctuate in an interval $(t_{\rm so}-\delta_{t_{\rm so}}, t_{\rm so}+\delta_{t_{\rm so}})$ with a uniform distribution. The fluctuation magnitude $\delta_{t_{\rm so}}$ increases from (a) 0.1Δ to (d) Δ.

to take place in the low chemical potential region. This feature can be observed from Fig. 4, which presents the phase diagrams of disordered QD-SC chains with increasing $\delta_{t_{\rm so}}$.

When the spin-flip hopping changes sign along the QD-SC chain, a pair of zero-energy fermionic bound states[39] arise at the interface between the neighboring domains with different signs of spin-flip hopping. These interface fermionic bound states can couple to other nearby bound states, including the MBS originally present at the ends of the QD-SC chain. These couplings can destroy the zero-energy MBS. To obtain a clear view of the interface fermionic bound states and their coupling to the MBS, we further consider a simple case where a short QD-SC chain possesses a constant spin-flip hopping on one half of the chain but a varying spin-flip hopping on the other half. Typically, we study a chain with 51 QDs connected by s-wave SCs. We set the spin-flip hopping between the neighboring QDs from the 1st to 26th sites as a constant $t_{\rm so}$, and adjust the spin-flip hopping $t_{\rm so}^a$ on the remaining part from $t_{\rm so}$ to $-t_{\rm so}$. In Fig. 5(a), we present the energy spectrum of such an inhomogeneous system versus the variation of the parameter $t_{\rm so}^a$, with the lowest six eigenstates close to zero plotted by curves. It is clearly shown that with the decrease and eventually the sign-inversal of $t_{\rm so}^a$, the bulk gap in the QD-SC chain gradually closes and the zero-energy fermionic bound states located around the 26th QD arise. Accordingly, the topological quantum number, Q, changes from -1 to 1 [refer to the open

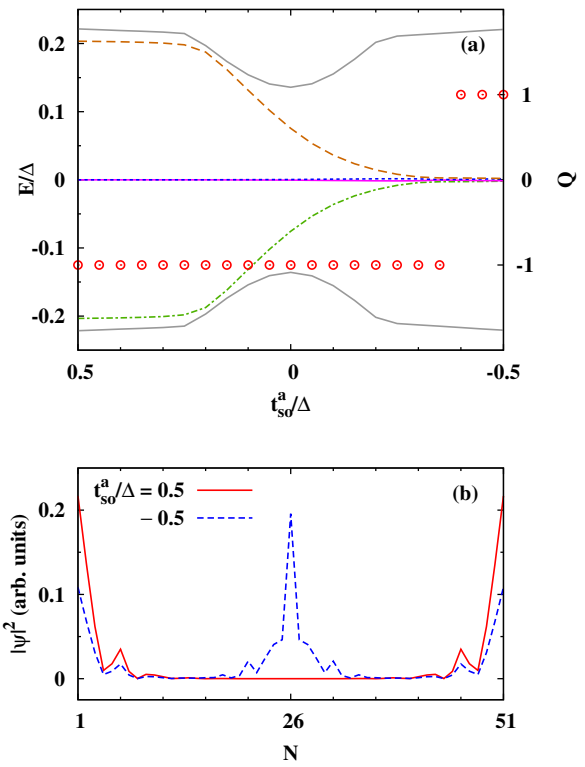

FIG. 5: (Color online) (a) Curves: energy spectrum (with only the lowest six eigenstates close to zero energy plotted) in an inhomogeneous QD-SC chain with a finite length (in the calculation we set the total number of QDs N to be 51), versus the variation of spin-flip hopping in one half of the QD chain $t^a_{\rm so}$. Circles: the topological quantum number Q [in Eq. (6)] of this inhomogeneous QD-SC chain (with the scale on the right-hand side of the frame), versus the variation of spin-flip hopping in one half of the QD chain $t^a_{\rm so}$. The spin-flip hopping in the other half of the QD-SC chain remains invariant as $t_{\rm so} = 0.5\Delta$. (b) Wave amplitude $|\Psi|^2$ of the state with its energy closest to zero. The solid curve stands for the weakly-coupled MBS in a homogeneous QD-SC chain where $t_{\rm so} = t^a_{\rm so} = 0.5\Delta$, while the dashed curve stands for the state where the MBS have disappeared due to their coupling to the interface fermionic bound states in an inhomogeneous QD-SC chain. For the homogeneous QD-SC chain, $t_{\rm so} = t^a_{\rm so} = 0.5\Delta$; while for the inhomogeneous QD-SC chain: $t_{\rm so} = -t^a_{\rm so} = 0.5\Delta$.

circles in Fig. 5(a)], indicating the disappearance of MBS due to their coupling to the fermionic bound states. In Fig. 5(b), we further present the wave amplitude of the lowest eigenstate, respectively for the cases with $t^a_{\rm so} = t_{\rm so}$ and $t^a_{\rm so} = -t_{\rm so}$. It is found that when $t^a_{\rm so} = t_{\rm so}$, i.e., the QD-SC chain is homogeneous, two weakly-coupled MBS are present. However, when $t^a_{\rm so} = -t_{\rm so}$, a state resulting from the coupling between MBS and the interface bound state replaces the original MBS.

V. CONCLUSION

In this work, we have studied the MBS in a disordered QD chain connected by s-wave SCs. We describe this one dimensional system by a tight-binding model. By calculating the topological quantum number based on the scattering matrix method, we can identify the topological property of such a QD-SC chain. In our study, we take into account disorder in both the spin-independent terms (including the chemical potential and the regular spin-conserving hopping) and the spin-independent term, i.e., the spin-flip hopping due to the Rashba SOC.

We find that the MBS are *not* completely immune to disorder in spin-independent terms, especially when the disorder is strong. Meanwhile, the Majorana bound states are relatively robust against disorder in the spin-flip hopping, as long as the spin-flip hopping is sign-ordered. Nevertheless, when the disorder induces sign-flip in spin-flip hopping, a topological-nontopological phase transition in the quantum dot chain tends to take place in the low chemical potential region. This study may provide insight into the search of MBS in solid-state systems.

Acknowledgments

The authors gratefully acknowledge E. Ya. Sherman and İ. Adagideli for valuable discussions and comments. P.Z. acknowledges the support of a JSPS Foreign Postdoctoral Fellowship under Grant No. P14330. F.N. is partially supported by the RIKEN iTHES Project, MURI Center for Dynamic Magneto-Optics via the AFOSR award number FA9550-14-1-0040, the IMPACT program of JST, and a Grant-in-Aid for Scientific Research (A).

Appendix A: Numerical scheme

As shown in Sec. III, the topological quantum number Q is determined by the reflection matrix R, which can be obtained by the transfer matrix M via Eq. (12). However, the recursive construction [i.e., Eq. (13)] is numerically unstable.[5,50] We stabilize it using the method described in Ref. 50. We briefly introduce this process here.

We label

$$M_n = \begin{pmatrix} a_n & b_n \\ c_n & d_n \end{pmatrix} \tag{A1}$$

and define

$$\mathscr{M}_n = \begin{pmatrix} \mathscr{A}_n & \mathscr{B}_n \\ \mathscr{C}_n & \mathscr{D}_n \end{pmatrix} = M_n M_{n-1} ... M_2 M_1. \tag{A2}$$

Here $\{a_n, b_n, c_n, d_n\}$ and $\{\mathscr{A}_n, \mathscr{B}_n, \mathscr{C}_n, \mathscr{D}_n\}$ are 4×4 sub-block matrices. In such framework, $M = \mathscr{M}_N$. Fur-

ther according to Eq. (12), we have $R = -\mathscr{D}_N^{-1}\mathscr{C}_N$ and $T = \mathscr{A}_N - \mathscr{B}_N\mathscr{D}_N^{-1}\mathscr{C}_N$.

Based on Eqs. (8) and (10), one finds that

$$M_n^\dagger \Sigma_z M_n = \Sigma_z,\ \Sigma_z = \begin{pmatrix} I & 0 \\ 0 & -I \end{pmatrix}. \tag{A3}$$

Therefore, one can construct a unitary matrix W_n from the non-unitary matrix M_n as

$$W_n = \begin{pmatrix} u_n & v_n \\ r_n & s_n \end{pmatrix} = \begin{pmatrix} -d_n^{-1}c_n & d_n^{-1} \\ a_n - b_n d_n^{-1} c_n & b_n d_n^{-1} \end{pmatrix}. \tag{A4}$$

Now let us define

$$\mathscr{W}_n = \begin{pmatrix} \mathscr{U}_n & \mathscr{V}_n \\ \mathscr{R}_n & \mathscr{S}_n \end{pmatrix} = W_n \odot W_{n-1} ... W_2 \odot W_1, \tag{A5}$$

where the operation $\odot$ is performed as

$$\begin{pmatrix} u_2 & v_2 \\ r_2 & s_2 \end{pmatrix} \odot \begin{pmatrix} u_1 & v_1 \\ r_1 & s_1 \end{pmatrix} = \begin{pmatrix} u_1 + v_1(1-u_2 s_1)^{-1} u_2 r_1 & v_1(1-u_2 s_1)^{-1} v_2 \\ r_2(1-s_1 u_2)^{-1} r_1 & s_2 + r_2(1-s_1 u_2)^{-1} s_1 v_2 \end{pmatrix}. \tag{A6}$$

In this way, $\mathscr{W}_n$ is the unitary counterpart of $\mathscr{M}_n$, i.e.,

$$\begin{pmatrix} \mathscr{U}_n & \mathscr{V}_n \\ \mathscr{R}_n & \mathscr{S}_n \end{pmatrix} = \begin{pmatrix} -\mathscr{D}_n^{-1}\mathscr{C}_n & \mathscr{D}_n^{-1} \\ \mathscr{A}_n - \mathscr{B}_n\mathscr{D}_n^{-1}\mathscr{C}_n & \mathscr{B}_n\mathscr{D}_n^{-1} \end{pmatrix}. \tag{A7}$$

As a result, for numerical stability, instead of calculating $\mathscr{M}_n$ by Eq. (A2), one can calculate the unitary matrix $\mathscr{W}_n$ based on Eq. (A5).

Finally, the topological quantum number Q can be obtained via the relation

$$Q = \mathrm{sgn\,Det}(R) = \mathrm{sgn\,Det}(-\mathscr{D}_N^{-1}\mathscr{C}_N) = \mathrm{sgn\,Det}(\mathscr{U}_N). \tag{A8}$$

[1] A.Y. Kitaev, Unpaired majorana fermions in quantum wires, Phys. Usp. **44**, 131 (2001).

[2] C.W.J. Beenakker, Search for Majorana Fermions in Superconductors, Annu. Rev. Con. Mat. Phys. **4**, 113 (2013).

[3] R.M. Lutchyn, J.D. Sau, and S. Das Sarma, Majorana Fermions and a Topological Phase Transition in Semiconductor-Superconductor Heterostructures, Phys. Rev. Lett. **105**, 077001 (2010).

[4] Y. Oreg, G. Refael and F. von Oppen, Helical Liquids and Majorana Bound States in Quantum Wires, Phys. Rev. Lett. **105**, 177002 (2010).

[5] T.P. Choy, J.M. Edge, A.R. Akhmerov, and C.W.J. Beenakker, Majorana fermions emerging from magnetic nanoparticles on a superconductor without spin-orbit coupling, Phys. Rev. B **84**, 195442 (2011).

[6] L. Fu and C.L. Kane, Superconducting Proximity Effect and Majorana Fermions at the Surface of a Topological Insulator, Phys. Rev. Lett. **100**, 096407 (2008).

[7] A. Cook and M. Franz, Majorana fermions in a topological-insulator nanowire proximity-coupled to an s-wave superconductor, Phys. Rev. B **84**, 201105 (2011).

[8] A.L. Rakhmanov, A.V. Rozhkov, and F. Nori, Majorana fermions in pinned vortices, Phys. Rev. B **84**, 075141 (2011).

[9] R.S. Akzyanov, A.V. Rozhkov, A.L. Rakhmanov, and F. Nori, Tunneling spectrum of a pinned vortex with a robust Majorana state, Phys. Rev. B **89**, 085409 (2014).

[10] R.S. Akzyanov, A.L. Rakhmanov, A.V. Rozhkov, and F. Nori, Majorana fermions at the edge of superconducting islands, Phys. Rev. B **92**, 075432 (2015).

[11] L. Jiang, D. Pekker, J. Alicea, G. Refael, Y. Oreg, A. Brataas, and F. von Oppen, Magneto-Josephson effects in junctions with Majorana bound states, Phys. Rev. B **87**, 075438 (2013).

[12] J.D. Sau and S. Das Sarma, Realizing a robust practical Majorana chain in a quantum-dot-superconductor linear array, Nat. Commun. **3**, 964 (2012).

[13] I.C. Fulga, A. Haim, A.R. Akhmerov, and Y. Oreg, Adaptive tuning of Majorana fermions in a quantum dot chain, New J. Phys. **15**, 045020 (2013).

[14] L. Dai, W. Kuo, and M.C. Chung, Extracting entangled qubits from Majorana fermions in quantum dot chains through the measurement of parity, Sci. Rep. **5**, 11188 (2015).

[15] L. Jiang, T. Kitagawa, J. Alicea, A.R. Akhmerov, D. Pekker, G. Refael, J.I. Cirac, E. Demler, M.D. Lukin, and P. Zoller, Majorana Fermions in Equilibrium and in Driven Cold-Atom Quantum Wires, Phys. Rev. Lett. **106**, 220402 (2011).

[16] V. Mourik, K. Zuo, S.M. Frolov, S.R. Plissard, and E.P.A.M. Bakkers, and L.P. Kouwenhoven, Signatures of Majorana Fermions in Hybrid Superconductor Semiconductor Nanowire Device, Science **336**, 1003 (2012).

[17] M.T. Deng, C.L. Yu, G.Y. Huang, M. Larsson, P. Caroff, and H.Q. Xu, Anomalous Zero-Bias Conductance Peak in a Nb-InSb Nanowire-Nb Hybrid Device, Nano Lett. **12**, 6414 (2012).

[18] A. Das, Y. Ronen, Y. Most, Y. Oreg, M. Heiblum, and H. Shtrikman, Zero-Bias Peaks and Splitting in an AlInAs Nanowire Topological Superconductor as a Signature of Majorana Fermions, Nat. Phys. **8**, 887 (2012).

[19] S.N. Perge, I.K. Drozdov, J. Li, H. Chen, S. Jeon, J. Seo, A.H. MacDonald, B.A. Bernevig, and A. Yazdani, Observation of Majorana Fermions in Ferromagnetic Atomic

Chains on a Superconductor, Science **346**, 602 (2014).

[20] J.P. Xu, M.X. Wang, Z.L. Liu, J.F. Ge, X.J. Yang, C.H. Liu, Z.A. Xu, D. Guan, C.L. Gao, D. Qian, Y. Liu, Q.H. Wang, F.C. Zhang, Q.K. Xue, and J.F. Jia, Experimental Detection of a Majorana Mode in the Core of a Magnetic Vortex inside a Topological Insulator-Superconductor $Bi_2Te_3/NbSe_2$ Heterostructure, Phys. Rev. Lett. **114**, 017001 (2015).

[21] C. Nayak, S.H. Simon, A. Stern, M. Freedman, and S. Das Sarma, Non-Abelian Anyons and Topological Quantum Computation, Rev. Mod. Phys. **80**, 1083 (2008).

[22] J. Alicea, Y. Oreg, G. Refael, F. von Oppen, and M.P.A. Fisher, Non-Abelian Statistics and Topological Quantum Information Processing in 1D Wire Networks, Nat. Phys. **7**, 412 (2011).

[23] S. Tewari, S. Das Sarma, C. Nayak, C. Zhang, and P. Zoller, Quantum Computation Using Vortices and Majorana Zero Modes of a $p_x + ip_y$ Superfluid of Fermionic Cold Atoms, Phys. Rev. Lett. **98**, 010506 (2007).

[24] M.W. Wu, J.H. Jiang, and M.Q. Weng, Spin Dynamics in Semiconductors, Phys. Rep. **493**, 61 (2010).

[25] S.N. Perge, S.M. Frolov, E.P.A.M. Bakkers, and L.P. Kouwenhoven, Spin-Orbit Qubit in a Semiconductor Nanowire, Nature **468**, 1084 (2010).

[26] P. Zhang, Z.L. Xiang, and F. Nori, Spin-orbit qubit on a multiferroic insulator in a superconducting resonator, Phys. Rev. B **89**, 115417 (2014).

[27] R. Li, J.Q. You, C.P. Sun, and F. Nori, Controlling a Nanowire Spin-Orbit Qubit via Electric-Dipole Spin Resonance, Phys. Rev. Lett. **111**, 086805 (2013).

[28] I. Buluta and F. Nori, Quantum Simulators, Science, **326**, 108 (2009).

[29] I. Buluta, S. Ashhab, and F. Nori, Natural and Artificial Atoms for Quantum Computation, Rep. Prog. Phys. **74**, 104401 (2011).

[30] J.Q. You and F. Nori, Atomic Physics and Quantum Optics Using Superconducting Circuits, Nature **474**, 589 (2011).

[31] L. Mao and C. Zhang, Robustness of Majorana modes and minigaps in a spin-orbit-coupled semiconductor-superconductor heterostructure, Phys. Rev. B **82**, 174506 (2010).

[32] D.A. Ivanov, Non-Abelian Statistics of Half-Quantum Vortices in p-Wave Superconductors, Phys. Rev. Lett. **86**, 268 (2001).

[33] A.A. Kovalev, A. De, and K. Shtengel, Spin Transfer of Quantum Information between Majorana Modes and a Resonator, Phys. Rev. Lett. **112**, 106402 (2014).

[34] P. Zhang and F. Nori, Coherent manipulation of a Majorana qubit by a mechanical resonator, Phys. Rev. B **92**, 115303 (2015).

[35] P.W. Brouwer, M. Duckheim, A. Romito, and F. von Oppen, Topological superconducting phases in disordered quantum wires with strong spin-orbit coupling, Phys. Rev. B **84**, 144526 (2011).

[36] P.W. Brouwer, M. Duckheim, A. Romito, and F. von Oppen, Probability Distribution of Majorana End-State Energies in Disordered Wires, Phys. Rev. Lett. **107**, 196804 (2011).

[37] Y. Hu, Z. Cai, M.A. Baranov, and P. Zoller, Majorana fermions in noisy Kitaev wires, Phys. Rev. B **92**, 165118 (2015).

[38] B. Pekerten, A. Teker, O. Bozat, M. Wimmer, and I. Adagideli, Disorder-induced topological transitions in multichannel Majorana wires, arXiv:1509.00449.

[39] J. Klinovaja and D. Loss, Fermionic and Majorana bound states in hybrid nanowires with non-uniform spin-orbit interaction, Eur. Phys. J. B **88**, 62 (2015).

[40] W. DeGottardi, D. Sen, and S. Vishveshwara, Majorana Fermions in Superconducting 1D Systems Having Periodic, Quasiperiodic, and Disordered Potentials, Phys. Rev. Lett. **110**, 146404 (2013).

[41] G. Goldstein and C. Chamon, Decay rates for topological memories encoded with majorana fermions, Phys. Rev. B **84**, 205109 (2011).

[42] D. Rainis and D. Loss, Majorana qubit decoherence by quasiparticle poisoning, Phys. Rev. B **85**, 174533 (2012).

[43] M.J. Schmidt, D. Rainis, and D. Loss, Decoherence of Majorana qubits by noisy gates, Phys. Rev. B **86**, 085414 (2012).

[44] J.C. Budich, S. Walter, and B. Trauzettel, Failure of protection of Majorana based qubits against decoherence, Phys. Rev. B **85**, 121405 (2012).

[45] M.M. Glazov, E. Ya. Sherman, and V. K. Dugaev, Two-dimensional electron gas with spin-orbit coupling disorder, Physica E **42**, 2157 (2010).

[46] P. Zhang and M.W. Wu, Electron spin relaxation in graphene with random Rashba field: comparison of the D'yakonov-Perel' and Elliott-Yafet-like mechanisms, New J. Phys. **14**, 033015 (2012).

[47] A.R. Akhmerov, J.P. Dahlhaus, F. Hassler, M. Wimmer, and C.W. J. Beenakker, Quantized Conductance at the Majorana Phase Transition in a Disordered Superconducting Wire, Phys. Rev. Lett. **106**, 057001 (2011).

[48] B.M. Fregoso, A.M. Lobos, and S. Das Sarma, Electrical detection of topological quantum phase transitions in disordered Majorana nanowires, Phys. Rev. B **88**, 180507 (2013).

[49] M. Gibertini, F. Taddei, M. Polini, and R. Fazio, Local density of states in metal-topological superconductor hybrid systems, Phys. Rev. B **85**, 144525 (2012).

[50] I. Snyman, J. Tworzydło, and C.W.J. Beenakker, Calculation of the conductance of a graphene sheet using the Chalker-Coddington network model, Phys. Rev. B **78**, 045118 (2008).